Mathematical morphology in non-Euclidean spaces and medical images -Technical report

Samy Blusseau

Mathematical morphology in non-Euclidean spaces and medical images - Technical report

Samy Blusseau

April, 2018

1 Lattice on the cone of semi positive definite matrices

1.1 Notations

- S_n: the set of $n \times n$ symmetric real valued matrices
- S_n^+: the set of semi-positive definite (SPD) matrices
- S_n^{++}: the set of positive definite matrices
- I_n: the identity matrix
- $tr(M)$: the trace of matrix M
- M^T: transposition of matrix M
- $||M||$: the Euclidean norm of matrix M, for the canonical scalar product $\langle A, B \rangle = tr(A^T B)$
- $\forall \lambda \in \mathbb{R}$, $T_\lambda = \{M \in S_n, tr(M) = \lambda\}$: the set of symmetric matrices with trace λ

1.2 The Loewner ordering is not a lattice ordering

Definition and geometric interpretation The Loewner ordering is defined on S_n as follows: for any $A, B \in S_n$,

$$A \geq B \iff A - B \in S_n^+.$$

If $A \in S_n^+$, it can be geometrically represented by an ellipsoid $\mathscr{E}_A = \{x \in \mathbb{R}^n, x^T Ax \leq 1\}$, the lengths of $\mathscr{E}_A$'s semi-axis being $1/\sqrt{\lambda_i(A)}$, if $\lambda_1, \dots, \lambda_n$ denote the eigenvalues of A (the ellipsoid can be degenerated, with infinitely long semi-axis when $\lambda_i = 0$). Then the Loewner ordering corresponds to a *reversed* inclusion ordering on ellipsoids: for $A, B \in S_n^+$,

$$A \geq B \iff \mathscr{E}_A \subseteq \mathscr{E}_B.$$

To get a more intuitive geometrical correspondance where the ellipsoid associated to the smaller element is included in the one associated to the bigger element, we can consider the ellipsoid whose semi-axis's lenghts are $\sqrt{\lambda_i}$. When $A \in S_n^{++}$ this corresponds to $\mathscr{E}_{A^{-1}}$, thus for $A, B \in S_n^{++}$,

$$A \geq B \iff A^{-1} \leq B^{-1} \iff \mathscr{E}_{B^{-1}} \subseteq \mathscr{E}_{A^{-1}},$$

and this can also be extended for non invertible matrices[1].

[1] I prefer not to spend more time on this since the Loewner ordering may not be what we need.

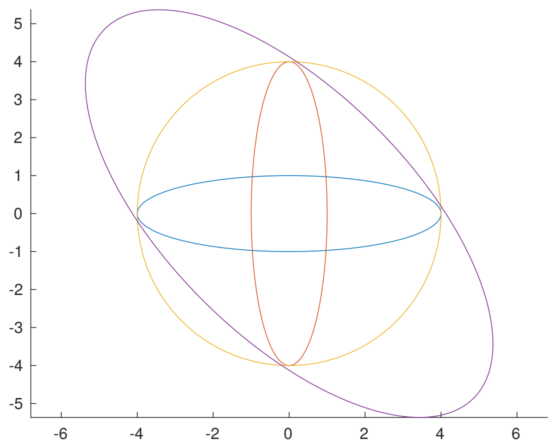

Figure 1: An example of minimal-volume enclosing ellipsoid (yellow), not comparable (in the Loewner sense) to another enclosing ellipsoid (in purple).

S_n^+ with the Loewner ordering is an anti-lattice An anti-lattice [4] is a poset in which, for any two elements A and B, a greatest lower bound exists if and only if A and B are comparable. In [4] Kadison shows that S_n with the Loewner ordering is an anti-lattice. Moreland and Gudder [5] proved that this is also true for S_n^+ (that is, a greatest lower bound exists *in* S_n^+ if and only if $A \geq 0$ and $B \geq 0$ are comparable), and Ando [1] generalizes the result to infinite dimension.

The misleading geometrical interpretation Despite the aforementioned results, one can argue that it is possible to find a unique smallest (largest) ellipsoid containing (contained in) a set of centered ellipsoids. The problem in this definition is that it refers to two different orderings: whereas the set of upper/lower bounds is defined by the Loewner ordering (or equivalently the inclusion ordering on ellipsoids), the smallest/biggest element of this set is defined by a *volume* total ordering. Unfortunately, the volume ordering does not induce the inclusion ordering, and one can find upper/lower bounds in the Loewner order that are not comparable with the "smallest"/"biggest" (in the volume sense) upper/lower bound - see Figure 1.

1.3 The (questionable) proposition of [2]

The authors of [2] acknowledge that the Loewner ordering is not a lattice ordering. However, the paper builds another ordering that is not proved to induce a lattice and that, in fact, seems to suffer from the same problem (the new order seems to be an anti-lattice as well).

In [2], computing the sup of a set of matrices in S_n^+ boils down to finding the smallest sphere covering a set of non centered spheres. As in the case of the ellipsoids, here two orderings are mixed: the inclusion ordering and the volume ordering. Again, we can find examples, as in Figure 2, where the resulting "smallest upper bound" is not comparable to other upper bounds in the ordering defined by the authors. These counter-examples seem to prove that this kind of ordering does not define a lattice. Indeed, if it did, the two blue spheres of Figure 2 would admit a unique sup. Since inclusion implies the ordering on volume, this sup would be the sphere of minimal volume enclosing the two blue spheres, that is the green sphere. The red sphere shows the existence of upper bounds not comparabale to the green one, and contradicts the existence of a unique minimal upper bound.

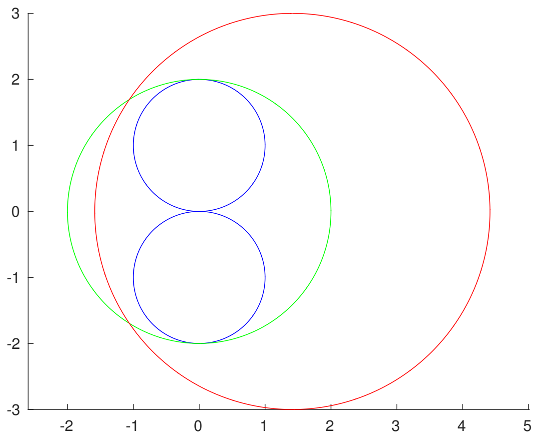

Figure 2: An example of minimal-volume enclosing ball (green), not comparable in the inclusion sense to another enclosing ball (red).

In the following I give a recap and reformulation of the construction presented in[2].

Bases of S_n^+ and their extreme points Figure 3 provides an illustration of the structure of the cone S_n^+, with the main features used for the construction of a new ordering in [2].

For any $\lambda \in \mathbb{R}$, we note $T_\lambda = \{M \in S_n, tr(M) = \lambda\}$. Then [2] recalls that $\mathscr{B}_1 := S_n^+ \cap T_1$, the set of positive matrices with trace 1, is a base of the cone S_n^+, that is to say: for any $M \in S_n^+, M \neq 0$, there exists a unique $\tilde{M} \in \mathscr{B}_1$ and a unique $\mu > 0$ such that $M = \mu \tilde{M}$. Indeed, here $\mu = tr(M)$ and $\tilde{M} = \frac{M}{tr(M)}$. Moreover, $\mathscr{B}_1$ is convex and its set of extreme points is known: it is the set of matrices $E_1 := \{vv^T, v \in \mathbb{R}^n, ||v|| = 1\}$. For a convex set $\mathscr{B}$, extreme points $ext(\mathscr{B})$ are defined as the points such that for any $x \in ext(\mathscr{B})$, $\mathscr{B} \setminus \{x\}$ is still convex, and they have the property to belong to the boundary of the convex set.

In this precise case, E_1 has another interesting property: its elements lie on the Euclidean sphere of centre $\frac{1}{n}I_n$ and radius $\sqrt{1-\frac{1}{n}}$: for any $M = vv^T \in E_1$, $||M - \frac{1}{n}I_n||^2 = tr((M - \frac{1}{n}I_n)^2) = tr(M^2) - \frac{2}{n}tr(M) + \frac{1}{n^2}tr(I_n) = tr(M) - \frac{1}{n} = 1 - \frac{1}{n}$.

Since extreme points are always included in the boundary of the convex set, and since $\mathscr{B}_1$ is a base of S_n^+, knowing $E_1 = ext(\mathscr{B}_1)$ gives a good idea of the general shape of the cone. Indeed, we can view $\mathscr{B}_1$ as some kind of convex polygone inscribed in the latter sphere, and then any “slice” $\mathscr{B}_\lambda = S_n^+ \cap T_\lambda$, $\lambda > 0$ can be deduced from $\mathscr{B}_1$ by homothety. We get that $\mathscr{B}_\lambda$ is also a base of S_n^+, its extremal points are exactly $\lambda \cdot E_1$, and they lie on the Euclidean sphere $\mathscr{S}_\lambda$ of center $\frac{\lambda}{n}I_n$ and radius $\lambda\sqrt{1-\frac{1}{n}}$. We note $\mathscr{C}_\lambda = \mathscr{S}_\lambda \cap T_\lambda$ the intersection of that sphere with T_λ.

The new cone [2] Just as $S_n^+ = \cup_{\lambda \geq 0} \mathscr{B}_\lambda$, a new cone C_n can be defined as $C_n = \cup_{\lambda \geq 0} \mathscr{C}_\lambda$. Although this is not explicit in the paper, the new ordering defined in [2] is the one induced by C_n:

$$A \geq B \iff A - B \in C_n.$$

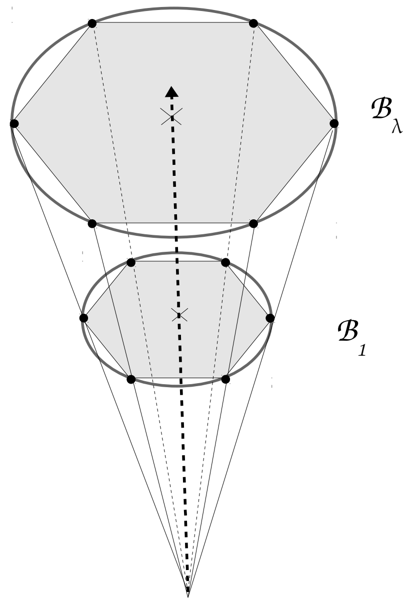

Figure 3: Illustration of the cone S_n^+. The gray polygones represent two bases of the cone, $\mathscr{B}_1$ and an arbitrary $\mathscr{B}_\lambda$ with $\lambda > 1$, intersections of the cone with the hyperplanes T_1 and T_λ. The extreme points of the bases are marked by black dots (there are infinitely many of them in reality), and the central dashed line indicates the span of the identity matrix I_n, orthogonal to each T_μ. On each base $\mathscr{B}_\mu$, the extreme points lie on a sphere $\mathscr{S}_\mu$ centered on $\frac{\mu}{n} I_n$ (marked by a black cross) and with radius $r_\mu = \mu\sqrt{1-\frac{1}{n}}$. Whereas S_n^+ is the union of all the gray polygones $\mathscr{B}_\mu$, the cone that defines the new ordering in [2] is the union of the $\mathscr{C}_\mu = \mathscr{S}_\mu \cap T_\mu$, $\mu \geq 0$.

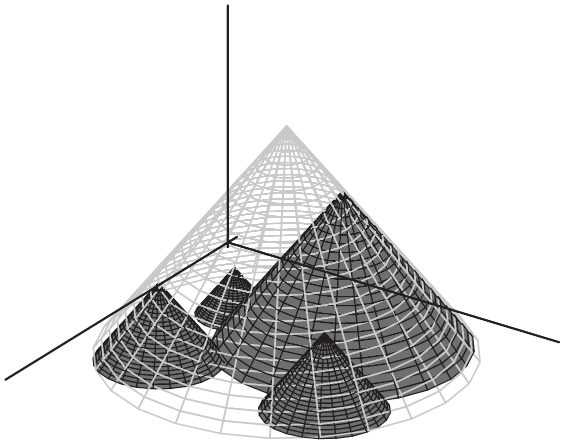

Figure 4: Examples of translated and reversed cones $M - C_n$ for several M. The light gray cone corresponds to the smallest ball $(M - C_n) \cap T_0$ containing all the others. Figure extracted from [2].

Readily, we have $S_n^+ \subseteq C_n$, which means that the Loewner ordering implies the new ordering. Furthermore, we get an easy characterization of C_n:

$$\begin{aligned} M \in C_n \quad &\Longleftrightarrow \quad M \in \mathscr{C}_{tr(M)} \\ &\Longleftrightarrow \quad ||M - \tfrac{tr(M)}{n} I_n|| \leq tr(M)\sqrt{1 - \tfrac{1}{n}} \\ &\Longleftrightarrow \quad tr(M^2) - \tfrac{1}{n} tr(M)^2 \leq tr(M)^2 (1 - \tfrac{1}{n}) \quad \text{and} \quad tr(M) \geq 0 \end{aligned}$$

$$M \in C_n \quad \Longleftrightarrow \quad ||M|| \leq tr(M).$$

Recalling that a matrix $M = \begin{bmatrix} a & c \\ c & b \end{bmatrix}$ is in S_2^+ if and only if $a \geq 0, b \geq 0$ and $det(M) \geq 0$, we can see that the Loewner ordering and the new ordering are equivalent for $n = 2$: $S_2^+ = C_2$.

In practice: inclusion ordering on spheres The ordering in [2] is directly defined in terms of inclusion of spheres. Using the notations introduced above, it can be written as

$$A \geq B \iff (B - C_n) \cap T_0 \subseteq (A - C_n) \cap T_0 \iff B - \mathscr{C}_{tr(B)} \subseteq A - \mathscr{C}_{tr(A)}.$$

$(B - C_n) \cap T_0$ is the intersection of the "ground" plane T_0, and the reversed cone $-C_n$ whose vertex has been placed in B (see Figure 4). It is therefore the sphere of T_0 centered in $m_B = B - \frac{tr(B)}{n} I_n$ and of radius $r_B = tr(B)\sqrt{1 - \frac{1}{n}}$. Similarly, $(A - C_n) \cap T_0$ is the sphere of T_0 centered in $m_A = A - \frac{tr(A)}{n} I_n$ and of radius $r_A = tr(A)\sqrt{1 - \frac{1}{n}}$. By applying a criterion on the distance between centres, we can check that this definition of the new ordering, based on the inclusion of spheres, is equivalent to the one we gave earlier:

$$\begin{aligned} A \geq B \quad &\Longleftrightarrow \quad ||m_A - m_B|| \leq r_A - r_B \\ &\Longleftrightarrow \quad ||A - B - \tfrac{tr(A-B)}{n} I_n|| \leq tr(A - B)\sqrt{1 - \tfrac{1}{n}} \\ &\Longleftrightarrow \quad ||A - B|| \leq tr(A - B) \\ &\Longleftrightarrow \quad A - B \in C_n. \end{aligned}$$

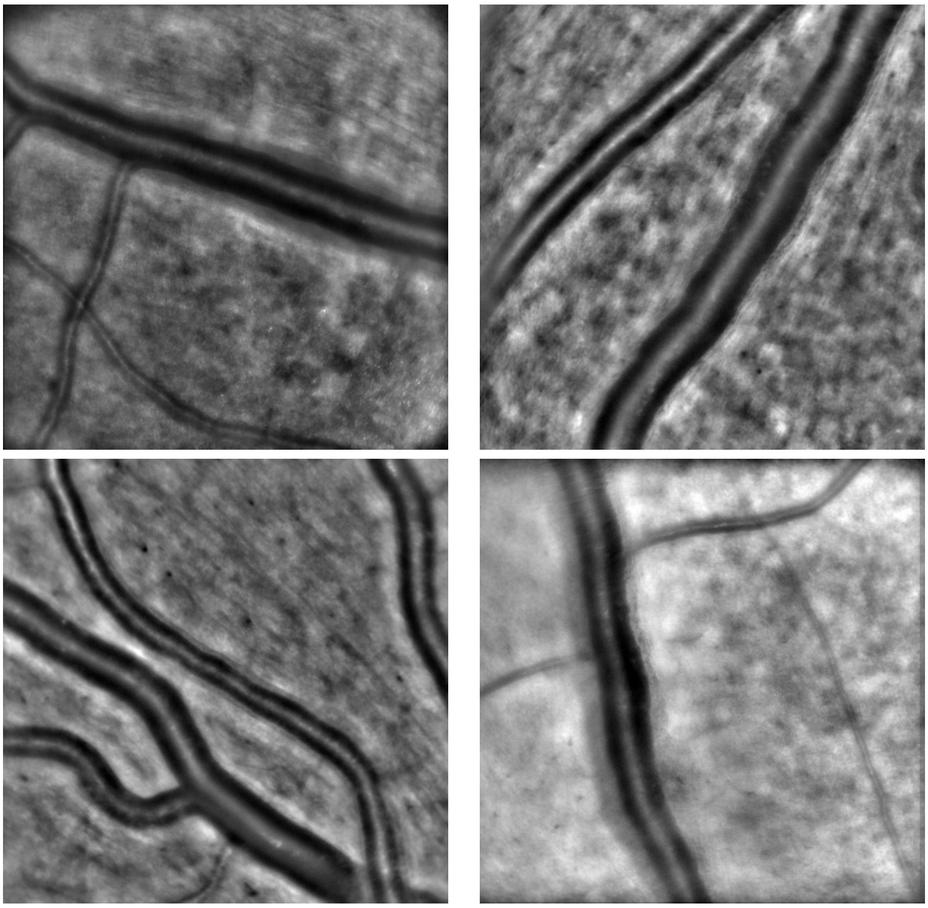

Figure 5: Example of input images.

Conclusion on [2] The paper proposes a new ordering but does not check whether it induces a lattice or not. From simple geometrical considerations it seems clear that it does not, and [6] asserts this ordering does not produce a lattice. I wonder if it is worth trying to show it is actually an anti-lattice.

This ordering and the definition of smallest upper bound may still be used as an approximation for morphological methods on S_n^+. The thesis [6] gives a quality measure of this approximation, I still need to have a look at it. However, it is not clear how it is better than the original Loewner ordering and the inclusion of centered ellipsoids. Therefore, if we decide to work with approximations of dilations and erosion, I would stay with the Loewner ordering.

2 Analysis of images of vessels based on structure tensors

2.1 Example of images

See Figure 5. In the following, we note f the image and suppose it is of size $N \times N$.

2.2 Structure tensor

The definition and computation of the structure tensor follows G. Peyré's numerical tour: `http://www.numerical-tours.com/matlab/pde_3_diffusion_tensor/`.

Gradient The following centered finite difference approximation of ∇f is used: $\nabla f(x,y) = (f_X(x,y), f_Y(x,y))^T$, where $f_X(x,y) = \frac{1}{2}(f(x+1,y) - f(x-1,y))$ for any y and $2 \le x \le N-1$, $f_X(1,y) = \frac{1}{2}(f(2,y) - f(N,y))$ and $f_X(N,y) = \frac{1}{2}(f(1,y) - f(N-1,y))$ (and similarly for $f_Y(x,y)$).

Tensor at scale zero The scale zero tensor T_0 maps each (x,y) to the symmetric matrix with rank ≤ 1

$$T_0(x,y) = \nabla f(x,y) \cdot \nabla f(x,y)^T = \begin{bmatrix} f_X(x,y)^2 & f_X(x,y)f_Y(x,y) \\ f_X(x,y)f_Y(x,y) & f_Y(x,y)^2 \end{bmatrix}.$$

It is straightforward that $\nabla f(x,y)$ is eigenvector of $T_0(x,y)$ with $||\nabla f(x,y)||^2$ as corresponding eigenvalue, and 0 is the other eigenvalue. Hence for any (x,y), $T_0(x,y)$ is an extreme point of the cone of positive semi-definite matrices S_2^+.

Tensor T_σ at scale $\sigma > 0$ It is a smoothed version of T_0, obtained by convolving the latter with the σ-scale Gaussian kernel

$$T_\sigma = G_\sigma T_0 = \begin{bmatrix} G_\sigma(f_X^2) & G_\sigma(f_X f_Y) \\ G_\sigma(f_X f_Y) & G_\sigma(f_Y^2) \end{bmatrix}$$

where G_σ is the smoothing operator. Note that, for any $u = (x,y)$, $T_\sigma(u)$ is a weighted sum of tensors $T_0(v)$ with positive weights, and is therefore a positive semi-definite matrix.

Eigen-decomposition of T_σ For each $u = (x,y)$, $T_\sigma(u)$ can be decomposed as

$$T_\sigma(u) = \lambda_1(u) e_1(u) \cdot e_1(u)^T + \lambda_2(u) e_2(u) \cdot e_2(u)^T$$

where $0 \le \lambda_2(u) \le \lambda_1(u)$ are $T_\sigma(u)$'s eigenvalues and $(e_1(u), e_2(u))$ its basis of orthogonal eigenvectors. If we represent $T_\sigma(u)$ by its corresponding ellipse

$$\mathscr{E}_u = \{X \in \mathbb{R}^2, X^T T_\sigma(u) X \le 1\}$$

then the main direction of $\mathscr{E}_u$ is given by the second eigenvector $e_2(u)$. For $\sigma = 0$, this vector is orthogonal to the gradient $\nabla f(u)$; more generally, for small σ, Peyré points out the Taylor expansion

$$T_\sigma(u) = T_0(u) + \sigma^2 H f(u)^2 + O(\sigma^3),$$

where Hf^2 is the Hessian of f^2. It is not clear what $e2(u)$ represents for larger σ, but it seems that inside a vessel the ellipse's main direction roughly coincides with the vessel's main direction.

Trace and anisotropy images (Figures 7 and 8) From the tensor field T_σ we can build two scalar images: the anisotropy image I_{an} and the trace image I_{tr}, respectively defined as

$$I_{an}(u) = 1 - \frac{2\lambda_2(u)}{tr(T_\sigma(u))} \quad \text{and} \quad I_{tr}(u) = tr(T_\sigma(u)) = \lambda_1(u) + \lambda_2(u).$$

We have $0 \le I_{an} \le 1$, and the closer $I_{an}(u)$ to 1, the more $T_\sigma(u)$ is anisotropic. I_{tr} can be seen as a smoothed version of the square norm of the ∇f.

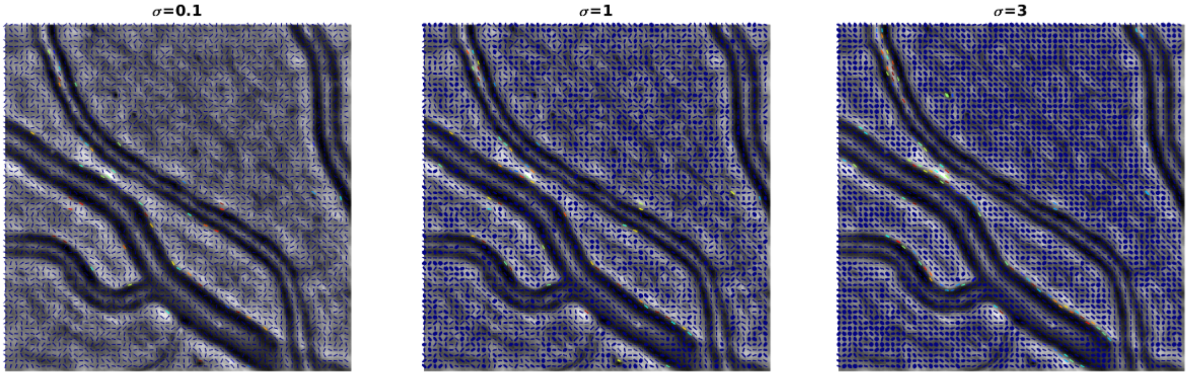

Figure 6: Structure tensors T_σ for the bottom left hand image of Figure, with $\sigma = 0.1$, $\sigma = 1$ and $\sigma = 3$. The shape of the represented ellipses show their anisotropy and main direction, whereas their colors must encode their trace (this is not clear yet).

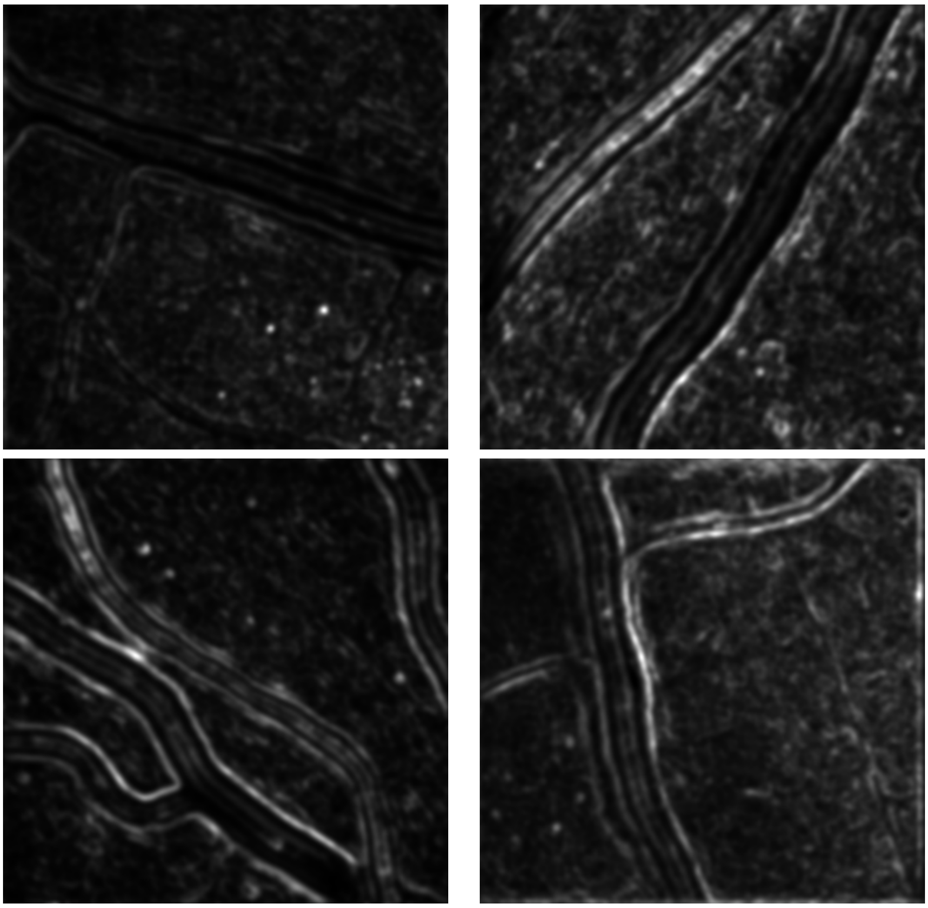

Figure 7: Trace images corresponding to the input of Figure 5, and the tensor field T_σ with $\sigma = 3$. They can be seen as smoothed version of the square norm of the ∇f.

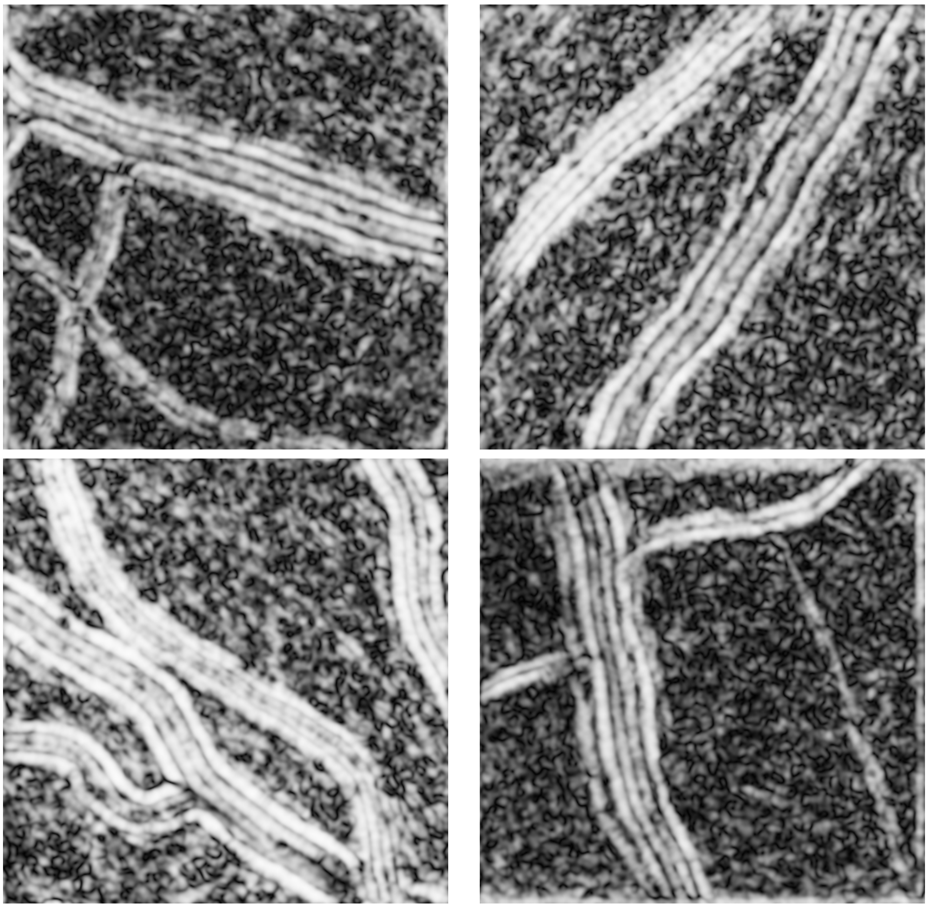

Figure 8: Anisotropy images corresponding to the input of Figure 5, and the tensor field T_σ with $\sigma = 3$. The closer $I_{an}(u)$ to 1, the more $T_\sigma(u)$ is anisotropic.

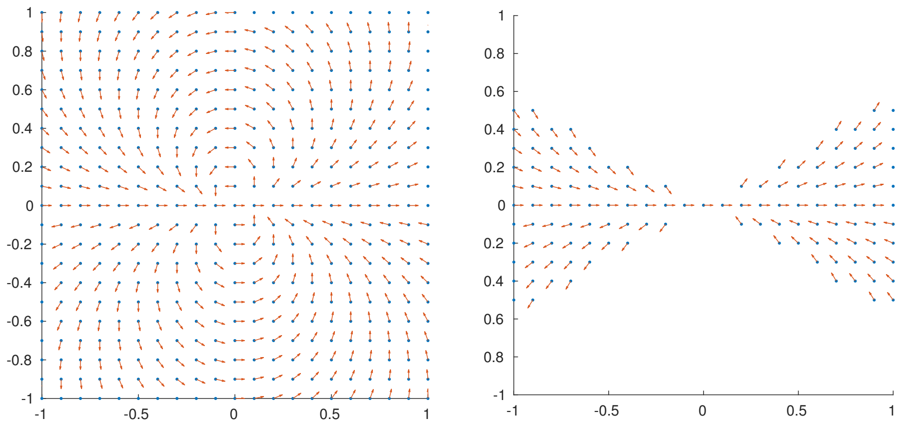

Figure 9: Left: a set of elements $(p, \overrightarrow{v})$ co-circular to the central element $(p_0, \overrightarrow{v_0})$ where p_0 is the origin and $v_0 = (1,0)^T$; Right: the elements form the left hand image that comply with the additional constraint that the (smaller) angle between the directions defined by $\overrightarrow{p_0 p}$ and $\overrightarrow{v}$ is smaller than $\frac{\pi}{6}$.

2.3 Structuring elements

Here we define for each pixel u the neighboorhood to be taken into account in the computation of flat dilation and erosion. The idea is to choose in a spatial window around u, those pixels v with for which the main orientation of $T_\sigma(v)$ is *consistent*, in some way, with $T_\sigma(u)$. So far I have used co-circularity as consistency criterion.

Co-circularity Given two points $p_1, p_2 \in \mathbb{R}^2$ and two vectors $\overrightarrow{v_1}, \overrightarrow{v_2}$, we say that $(p_1, \overrightarrow{v_1})$ and $(p_2, \overrightarrow{v_2})$ are co-circular if there is a circle tangent in p_1 and p_2 to $\overrightarrow{v_1}$ and $\overrightarrow{v_2}$ respectively. An infinite radius for the circle corresponds to the case when $\overrightarrow{p_1 p_2}$, $\overrightarrow{v_1}$ and $\overrightarrow{v_2}$ are colinear, which we consider a particular case of cocircularity.

Additional constraint As shown on the left of Figure 9, co-circularity allows "ladder" configurations, which we may want to discard in the following. If so, one can impose an additional constraint, namely that the angle between $\overrightarrow{p_1 p_2}$ and $\overrightarrow{v_2}$ is below a certain threshold.

Neighbourhood graph From the above we define an (undirected) graph (G,E) as follows: the set of nodes G is the set of pixels in the image $\{u_1, u_2, \ldots, u_{N^2}\}$; $(u_i, u_j) \in E$ iff u_j is in a square window of fixed size $2p+1$, centered on u_i (that is, $||u_i - u_j||_\infty \leq p$), and $(u_i, e_2(u_i))$ and $(u_j, e_2(u_j))$ are co-circular up to a certain angular tolerance, with the additional constraint described earlier to avoid ladder configurations - see Figure 9.

2.4 Morphological filters

Max-plus convolution Building on the graph (G,E) of the previous section, let W the $N^2 \times N^2$ adjacency matrix defined by $W_{ij} = 1 \iff (u_i, u_j) \in E$ or $i = j$, and $W_{ij} = 0$ otherwise. It encodes the structuring elements for any pixel, and we can now use it to compute max-plus convolutions (dilations

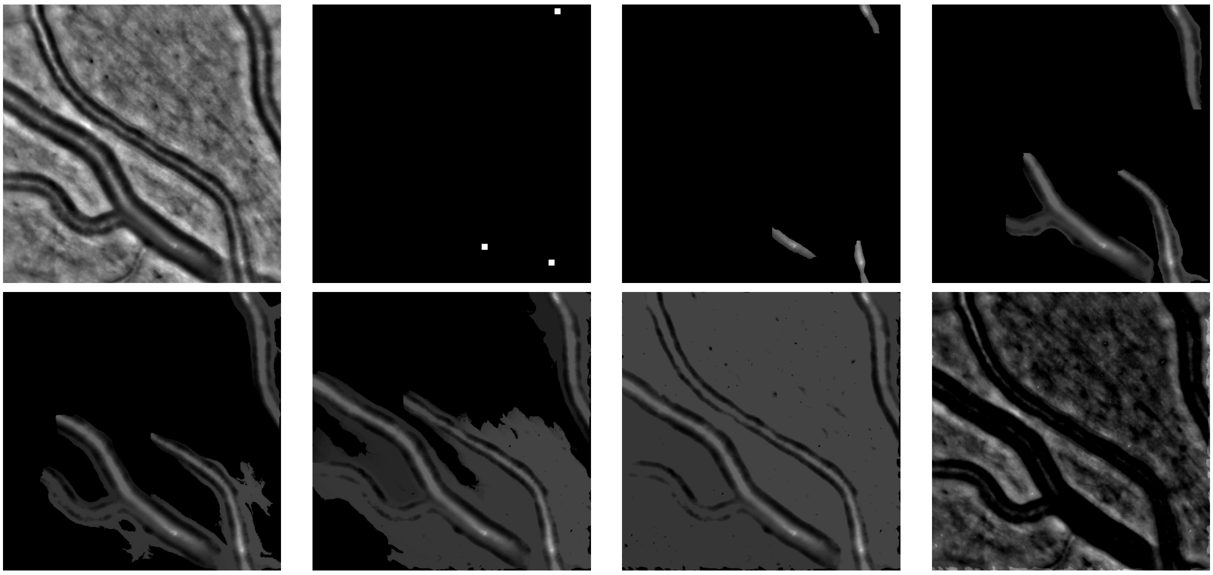

Figure 10: Illustration of the geodesic reconstruction by dilation. From left to right, top to bottom: mask image I (in this case, the original image); marker image R (defined manually); I_5, I_{25}, I_{35}, I_{50}, final reconstruction $\tilde{I} = I_{178}$; residual image $I - \tilde{I}$.

and erosions) on any sclar image I of size $N \times N$ [7]:

$$\delta(I)(u_i) = \bigvee_j \Big(I(u_j) + \log(W_{ij}) \Big) \quad \text{and} \quad \varepsilon(I)(u_i) = \bigwedge_j \Big(I(u_j) - \log(W_{ji}) \Big). \tag{1}$$

In particular, I can be the original image f, the anisotropy image or the trace image (Figures 5, 7 and 8).

Geodesic reconstruction by dilation We want to reconstruct a structure in an image I, e. g. a vessel, and possibly only this structure. If the structure is bright on a darker background, a possible strategy is to start from a marker image R representing a small part of the structure, and dilate it recursively under the constraint that the produced image remains smaller than I. By doing so, we hope to recover the bright structure as it is in I, while the background should remain relatively flat and smaller than it is in I.

More formally, given a mask image I and a marker image R, both $N \times N$, the geodesic reconstruction by dilation consists in building recursively a sequence of images $(I_n)_{n \geq 0}$,

$$I_0 = R \wedge I \quad \text{and} \quad I_{n+1} = \delta(I_n) \wedge I,$$

and finally take the sup $\tilde{I} = \bigvee_{n \geq 0} I_n$. Since in our case $W_{ii} = 1$, the dilation is extensive: $\delta(I)(u_i) \geq I(u_i)$, and the sequence $(I_n)_{n \geq 0}$ is increasing. Furthermore, $I_n \leq I$ for any n, hence the sequence converges to its maximal element $I_{n_{\max}}$ after a finite number $n_{\max}$ of iterations, producing the final reconstruction $\tilde{I} = I_{n_{\max}}$.

Figure 10 shows an example of such a reconstruction, in which the mask image I is an original image of vessels, and the markers have been defined manually to match bright regions in the vessels. The structuring elements (or equivalently the adjacency matrix W) was calculated on the tensor field T_σ associated with the original image, with $\sigma = 3$.

Ideas

- In the geodesic reconstruction, the mask image could be the anisotropy or trace image as well. Interestingly, they are independent on the contrast (it should work for bright vessels on dark background as well as for dark vessels on bright background). I have tried to work with the anisotropy but it is quite a noisy image and the reconstruction is not very accurate with respect to the original shape of the vessel - more work needs to be done on that. Experiments with the trace are on going as well.
- In the definition of the structuring elements, more information can be included than the spatial and angular consistency.I have tried to include the trace information, to avoid the existence of a path between pixels inside a vessel and pixels outside a vessel. So far this has not really worked out.
- The good part of working with the tensor field T_σ is that it provides positive semi-definite matrices, on which we can test methods to be adapted later on diffusion tensors. However, it raises some issues regarding the analysis of vessel images. First, it contains a scale parameter σ, which means that either a multi-scale approach or an automatic scale definition is required. Second, as said earlier, a structure tensor $T_\sigma(u)$ is merely a weighted sum of (rank 1) positive semi-definite matrices. It is not clear how this averaging behaves with respect to orientation information, especially in bifurcations.
- It seems that Frangi's vessel enhancement [3], based on the analysis of the Hessian, gives accurate segmentation of vessels. It may be interesting to figure out how our approach can add to Frangi's.
- As suggested in previous discussions, we should compare the results obtained with our definition of the structuring elements, to more classic ones (non-adaptive structuring elements, sets of differently oriented segments as structuring elements...).

3 Tropical and morphological operators for signal on graphs

This section aims at setting or recalling ([7]) some results about morphological operators for signals on graphs, defined as max/min-plus convolutions as in Equation 1. These results may help to get an insight on all the operators we will define based on this setting.

3.1 Setting and definitions

The first two definitions are taken from [7], and deal with a class of real matrices W.

Definition 1 (Morphological weight matrix). *A $N \times N$ real matrix $W = (w_{ij})_{1\leq i,j\leq N}$ is called a morphological weight matrix if $-\infty \leq w_{ij} \leq 0$ for any $(i,j), 1 \leq i,j \leq N$.*

Definition 2 (Conservative morphological weight matrix). *A morphological weight matrix W is said* conservative *if $w_{ii} = 0$ for any $i, 1 \leq i \leq N$.*

We consider a weighted and directed graph $G = (V,E)$ containing N nodes, whose $N \times N$ adjacency matrix, noted W, is a morphological weight matrix:

$$\begin{cases} -\infty < w_{ij} \leq 0 & \text{if } (i,j) \in E \\ w_{ij} = -\infty & \text{if } (i,j) \notin E. \end{cases}$$

Note this can be interpreted as taking the log of weights in $[0,1]$, where the absence of edge from node i to node j would be represented by $w_{ij} = 0$.

Definition 3 (Path). *We call path from node i to node j in G, a tuple of nodes $(k_1,\dots,k_n)$ such that $k_1 = i$, $k_n = j$, and $(k_p,k_{p+1}) \in E$ (or equivalently $w_{k_pk_{p+1}} > -\infty$) for $1 \leq p \leq n-1$.*

We will note Γ_{ij} the set of paths from i to j in G, and $\Gamma_{ij}^{(p)}$ the set of paths from i to j in G containing at most p nodes, for $p \geq 1$.

Definition 4 (Weight of a path)**.** *Given the weight matrix W, the weight of a path $\gamma = (k_1, \dots, k_n)$ in G, noted $\omega(\gamma)$, is the sum $\omega(\gamma) = \sum_{p=1}^{n-1} w_{k_p k_{p+1}}$.*

It is easy to see that the set $\{\omega(\gamma), \gamma \in \Gamma_{ij}\}$ has a maximum value whenever Γ_{ij} is non empty. Indeed every $w_{k_p k_{p+1}}$ is non positive, and so is the weight of a path. Hence, for a non-empty set of paths Γ_{ij}, the set $\{\omega(\gamma), \gamma \in \Gamma_{ij}\}$ has a least upper bound, noted $\omega^*(\Gamma_{ij})$. Clearly, Γ_{ij} must contain at least a path without a cycle (that is, in which a node is present at most once). Noting Γ'_{ij} the set of paths without a cylce in Γ_{ij}, then Γ'_{ij} is non empty and we notice that $\omega^*(\Gamma_{ij}) = \omega^*(\Gamma'_{ij})$. This is because one can associate to any path with a cycle a path without a cycle, and the latter has a larger weight. Since Γ'_{ij} is finite (it contains no more than $(N-2)!$ paths), $\omega^*(\Gamma'_{ij})$ is a maximum, achieved by a at least a path $\gamma^* \in \Gamma'_{ij}$. Since $\Gamma'_{ij} \subset \Gamma_{ij}$, $\omega^*(\Gamma_{ij})$ is also a maximum. It follows that there is a maximal weight for any non empty set of paths, which allows Definition 5.

Definition 5 (Maximal weight, maximal path)**.** *We call* maximal weight *for a non-empty set of paths Γ the number*

$$\omega^*(\Gamma) := \max_{\gamma \in \Gamma} \omega(\gamma).$$

Then a maximal path *in Γ is a path $\gamma^* \in \Gamma$ such that $\omega(\gamma^*) = \omega^*(\Gamma)$, i.e. achieving the maximal weight among the paths in Γ.*

For completeness, we will use the convention $\omega^*(\emptyset) = -\infty$.

Now, let $x = (x_1, \dots, x_N)$ a signal on G, with values in the lattice $L = ([0,1], \leq)$. We define its dilation and erosion induced by W as

$$\forall i \in \{1, \dots, N\}, \quad \delta_W(x)_i = \bigvee_{j=1}^{N} \Big(x_j + w_{ij}\Big) \quad \text{and} \quad \varepsilon_W(x)_i = \bigwedge_{j=1}^{N} \Big(x_j - w_{ji}\Big). \tag{2}$$

As max-plus products, the dilation δ_W and erosion ε_W may be noted:

$$\delta_W(x) \doteq Wx \quad \text{and} \quad \varepsilon_W(x) \doteq 1 - \Big(W^T(1-x)\Big).$$

Similarly, we will note W^2 the max-plus product of W by itself, that is

$$(W^2)_{ij} = \bigvee_{k=1}^{N} \Big(w_{ik} + w_{kj}\Big),$$

and more generally W^p the p-th power of W in the max-plus sense, for any integer $p \geq 0$ (for $p = 0$, W^p is the max-plus identity matrix, for which $w_{ii} = 0$ and $w_{ij} = -\infty$ for $i \neq j$).

Finally, since $-\infty$ is the neutral element for the max operator and is absorbant for the sum, only the terms for which $w_{ij} > -\infty$ count in the previous definition of dilation (Eq. 2), that is to say only the nodes j for which $(i,j) \in E$ - the neighbours of i in G. The same remark holds for the erosion, replacing max by min and switching i and j. We will note $\mathcal{N}_i \doteq \Big\{ j \in \{1, \dots, N\}, (i,j) \in E \Big\}$ the set of neighbours of i in G. Then as we just noticed

$$\delta_W(x)_i = \bigvee_{j \in \mathcal{N}_i} \Big(x_j + w_{ij}\Big) \quad \text{and} \quad \varepsilon_W(x)_i = \bigwedge_{j, i \in \mathcal{N}_j} \Big(x_j - w_{ji}\Big).$$

In all the remaining, we will always assume $i \in \mathcal{N}_i$, with $w_{ii} = 0$. In other words, we assume W is a conservative morphological weight matrix (See Definitions 1 and 2).

3.2 Properties of W^p

Proposition 1. *Let W a conservative morphological weight matrix and $G = (V,E)$ the associated graph. Then for any $p \in \mathbb{N}$, $1 \le i,j \le N$,*

1. *$(W^p)_{ij} > -\infty$ if and only if there is at least a path from node i to node j in G containing at most $p+1$ node(s) (i.e. iff $\Gamma_{ij}^{(p+1)}$ is non empty)*
2. *$(W^p)_{ij}$ is the maximal weight of the set of paths from node i to node j containing at most $p+1$ node(s): $(W^p)_{ij} = \omega^*(\Gamma_{ij}^{(p+1)})$.*

At this point one should remember that the w_{ij} are non positive, $w_{ij} = 0$ modeling the strongest possible effect of node i on node j and $w_{ij} = -\infty$ meaning no effect at all. Therefore, a large weight $\omega(\gamma)$ for path $\gamma \in \Gamma_{ij}$ represents a strong link from node i to node j.

Proof. Note that once point 1 is proven[2], we only need to prove point 2 in the case where $(W^p)_{ij} > -\infty$. Indeed if $(W^p)_{ij} = -\infty$ then, according to point 1, $\Gamma_{ij}^{(p+1)} = \emptyset$ and by convention $\omega^*(\Gamma_{ij}^{(p+1)}) = -\infty = (W^p)_{ij}$.

The case $p = 0$ is clear although not very informative. There is a path from i to j containing at most $p+1 = 1$ node if and only if $i = j$, and if so there is only one path of weight $w_{ii} = 0$. Recall that W^0 is the max-plus identity matrix, for which indeed $(W^0)_{ij} = -\infty$ if $i \ne j$ and $(W^0)_{ii} = 0$.

We assume the proposition true for a given $p \ge 0$. By definition

$$(W^{p+1})_{ij} = (W^p W)_{ij} = \bigvee_{k=1}^{N} \Big((W^p)_{ik} + w_{kj} \Big).$$

Hence $(W^{p+1})_{ij} > -\infty$ if and only if, for at least one k, $(W^p)_{ik} > -\infty$ and $w_{kj} > -\infty$, which means there is a path from i to k containing at most $p+1$ nodes, and an edge from k to j, and therefore at least one path from i to j containing $p+2$ nodes. This shows point 1.

Now we suppose $(W^{p+1})_{ij} > -\infty$. By assumption $(W^p)_{ik}$ is optimal for any k reachable from i along a path containing at most $p+1$ nodes. Then the optimality of $\bigvee_{k=1}^{N} \Big((W^p)_{ik} + w_{kj} \Big)$ among the paths of $\Gamma_{ij}^{(p+2)}$ is a consequence of a classical dynamic programming argument. $\square$

Remark Interestingly, W^p is also a conservative morphological weight matrix. Its corresponding graph, that we note G^p, can be seen as the original graph G to which a direct edge has been added between nodes i and j whenever there is a path containing at most $p+1$ nodes from i to j in G. The weight associated with this new edge is $(W^p)_{ij} = \omega^*(\Gamma_{ij}^{(p+1)})$, the maximal weight for the paths from i to j containing at most $p+1$ nodes.

Corollary 1. *Let W a $N \times N$ conservative morphological weight matrix. Then $W^N = W^{N-1}$ and therefore there exists an integer $p_{max} = \min\{p \in \mathbb{N}, W^p = W^{p+1}\}$.*

Proof. This result is a direct consequence of the interpretation of $(W^N)_{ij}$ as the length of the largest path from i to j contanining at most $N+1$ nodes. Since the graph contains N nodes, the latter path actually contains at most N nodes and therefore $(W^N)_{ij} = (W^{N-1})_{ij}$. This shows that the set of integers p such that $W^p = W^{p+1}$ is not empty and as such has a smallest element p_{max}. $\square$

[2]Point 1 can be inferred from a classical graph theory result on the powers (in the usual algebra this time) of the adjaceny matrix, and taking the *log*. We will nevertheless prove it here too.

We will note $W^\infty \doteq W^{p_{max}} = W^{N-1}$. It is clear from Proposition 1 that $(W^\infty)_{ij} > -\infty$ if and only if there is a path from i to j, and $(W^\infty)_{ij}$ is the maximal weight for the paths from i to j: $(W^\infty)_{ij} = \omega^*(\Gamma_{ij})$.

Corollary 2. *Let W a conservative morphological weight matrix, and $p \in \mathbb{N}$. Then $(W^T)^p = (W^p)^T$.*

Proof. Again, this is clear from the graph interpretation. If $G = (V,E)$ is the graph associated with W, we note $G' = (V,E')$ the graph associated with W^T. G' has the same nodes as G but its edges are reversed with respect to G: $(i,j) \in E \iff (j,i) \in E'$, and the associated weight is the same. Threfore, since $(W^T)^p_{ij}$ is the maximal weight for the paths in G' from i to j containing at most $p+1$ nodes, it is also the maximal weight for the paths in G from j to i containing at most $p+1$ nodes. Hence $(W^T)^p_{ij} = (W^p)_{ji}$, and this holds for any (i,j). $\square$

Note that the result can also be shown by induction exactly like in the linear matrix power case. Indeed, here $+$ law verify the same sufficient conditions as the $\times$ law in the linear case: it is associative and commutative.

3.3 Operators and filters

From now on, W is a $N \times N$ conservative morphological weight matrix, and the coefficient on the i-th row and j-th column of the matrix W^p (noted $(W^p)_{ij}$ in the previous section) will be noted $w^{(p)}_{ij}$. The graph associated with W is noted $G = (V,E)$ and the one associated with W^p is noted $G^p = (V,E^p)$.

3.3.1 Iterated erosions and dilations

As it is well known in mathematical morphology, if a dilation δ and an erosion ε form an adjunction, then $\delta^p = \delta \circ \cdots \circ \delta$ and $\varepsilon^p = \varepsilon \circ \cdots \circ \varepsilon$ are also adjoint dilation and erosion. The associativity of the max-plus product of matrices yields the following result for the dilation and erosion defined by Eq. 2.

Proposition 2. *Let W a conservative morphological weight matrix, and $p \in \mathbb{N}$. Then $\delta^p_W = \delta_{(W^p)}$ and $\varepsilon^p_W = \varepsilon_{(W^p)}$.*

Proof. For the dilation, it is a direct consequence of the max-plus product associativity. For the erosion, we can use the fact that $(\varepsilon_W)^p(x) = 1 - (\delta_{W^T})^p(1-x)$ and that $(W^T)^p = (W^p)^T$. $\square$

A consequence of this is that we can simply express the iterated erosions and dilations as

$$\forall i \in \{1,\ldots,N\}, \quad \delta^p_W(x)_i = \bigvee_{j=1}^{N} \left(x_j + w^{(p)}_{ij} \right) \quad \text{and} \quad \varepsilon^p_W(x)_i = \bigwedge_{j=1}^{N} \left(x_j - w^{(p)}_{ji} \right), \tag{3}$$

where, as shown earlier, $w^{(p)}_{ij}$ represents the strongest link from i to j among the paths containing at most $p+1$ nodes. Another consequence is the semi-group property: $\delta_{(W^p)}\delta_{(W^q)} = \delta_{(W^{p+q})}$.

Extensivity, anti-extensivity Since W and any of its max-plus powers W^p are conservative morphological weight matrices, it follows that δ^p_W is extensive and ε^p_W is anti-extensive for any $p \geq 0$. This holds for $\varepsilon^\infty_W = \varepsilon^{p_{max}}_W$ and $\delta^\infty_W = \delta^{p_{max}}_W$. A consequence is that $\delta^\infty_W \varepsilon^\infty_W = \varepsilon^\infty_W$ and $\varepsilon^\infty_W \delta^\infty_W = \delta^\infty_W$.

Invariant nodes For a signal x on G and any $p \geq 0$ or $p = \infty$, we note $F_p(x) \doteq \{i \in V, \varepsilon_W^p(x)_i = x_i\}$ and $F'_p(x) \doteq \{i \in V, \delta_W^p(x)_i = x_i\}$ the sets of nodes invariant under ε_W^p and δ_W^p respectively.

Proposition 3. *For a signal x and any $0 \leq p \leq \infty$, the sets $F_p(x)$ and $F'_p(x)$ are non-empty.*

Proof. We prove the case of $F_p(x)$, the other one is then obtained by duality. The anti-extensivity of ε_W^p yields $\varepsilon_W^p(x)_{i_0} < x_{i_0}$ for any node i_0 that is not in $F_p(x)$. From equation 3, we deduce the existence of a node i_1 such that $\varepsilon_W^p(x)_{i_0} = x_{i_1} - w_{i_1 i_0}^{(p)} \geq x_{i_1}$. Therefore, $i_1 \neq i_0$ and $x_{i_0} > x_{i_1}$. If $F_p(x)$ were empty, we could proceed likewise to order the N values of x into a decreasing sequence $x_{i_0} > x_{i_1} > \cdots > x_{i_N}$. But then x_{i_N} must be in $F_p(x)$ otherwise there would be a node j such that $x_{i_N} > x_j$, which would contradict the previous ordering. $\square$

Idempotence of ε_W^∞ and δ_W^∞ This is straightforward from Corollary 1: $\varepsilon_W^{p_{max}} = \varepsilon_W^{p_{max}+1} = \varepsilon_W^\infty$. The erosion and dilation ε_W^∞ and δ_W^∞ are therefore morphological filters, and this is one of the reasons for studying them.

We will now focus on ε_W^∞ but what follows holds for δ_W^∞ by duality. The following result gives an idea of what ε_W^∞ should look like.

Proposition 4. *Let x a signal on G. For any node i, there is a node $j \in F_\infty(x)$ such that*

$$\varepsilon_W^\infty(x)_i = x_j - w_{ji}^{(\infty)}$$

and for any node k on a path from i to j achieving $w_{ji}^{(\infty)}$,

$$\begin{cases} \varepsilon_W^\infty(x)_k &= \quad x_j - w_{jk}^{(\infty)} \\ \varepsilon_W^\infty(x)_i &= \quad \varepsilon_W^\infty(x)_k - w_{ki}^{(\infty)}. \end{cases}$$

This means that the tranformed signal $y = \varepsilon_W^\infty(x)$ is composed of some minima $y_{j_0} = x_{j_0}, j_0 \in F_\infty(x)$, and increasing sequences $y_{j_0} \leq y_{j_1} \leq \cdots \leq y_{j_k}$ along "strong" paths of G, each step between two consecutive values being exactly $y_{j_{p+1}} - y_{j_p} = w_{j_p j_{p+1}}^{(\infty)} = w_{j_p j_{p+1}}$.

Proof. Let us start with the first statement. Let $i \in V$ be a node of G.
Case 1: $i \in F_\infty(x)$.
Then we already have the result: $\varepsilon_W^\infty(x)_i = x_i = x_i - w_{ii}^{(\infty)}$.
Case 2: $i \notin F_\infty(x)$.
Then there is a node $j \neq i$ such that $\varepsilon_W^\infty(x)_i = x_j - w_{ji}^{(\infty)}$, and we need to show that $j \in F_\infty(x)$. Assume the contrary, that $j \notin F_\infty(x)$. Then there is a node $j' \neq j$ such that $\varepsilon_W^\infty(x)_j = x_{j'} - w_{j'j}^{(\infty)} < x_j$, the last inequality coming from the anti-extensitvity of ε_W^∞ and the fact that $\varepsilon_W^\infty(x)_j \neq x_j$ by assumption.
Then we get

$$\varepsilon_W^\infty(x)_i = x_j - w_{ji}^{(\infty)} > x_{j'} - w_{j'j}^{(\infty)} - w_{ji}^{(\infty)}.$$

But $w_{j'j}^{(\infty)} + w_{ji}^{(\infty)}$ is the weight of a path from i to j in G, and as such it is not larger than $w_{ji}^{(\infty)}$, the largest weight of a path from i to j. So $-w_{j'j}^{(\infty)} - w_{ji}^{(\infty)} \geq -w_{ji}^{(\infty)}$ and therefore

$$\varepsilon_W^\infty(x)_i > x_{j'} - w_{j'i}^{(\infty)}$$

which contradicts the expression of $\varepsilon_W^\infty(x)_i$ as an infimum: $\varepsilon_W^\infty(x)_i = \bigwedge_{k=1}^N \left(x_k - w_{ki}^{(\infty)}\right)$.
For the second statement, let k a node on a path from i to j achieving $w_{ji}^{(\infty)}$. By the same argument as just above, if we assume that $\varepsilon_W^\infty(x)_k = x_{j'} - w_{j'k}^{(\infty)} \neq x_j - w_{jk}^{(\infty)}$ for a certain $j' \neq j$, then we find again that $\varepsilon_W^\infty(x)_i > x_{j'} - w_{j'i}^{(\infty)}$. This proves the first line of the second statement, and the second line is then the consequence of the equality $w_{ji}^{(\infty)} = w_{jk}^{(\infty)} + w_{ki}^{(\infty)}$ when k is a node on a path from i to j achieving $w_{ji}^{(\infty)}$. $\square$

An implication of Proposition 4 is that $\varepsilon_W^\infty(x)$ is fully determined by its values on $F_\infty(x)$, in the following sense. Given a signal $y \geq \varepsilon_W^\infty(x)$ such that y coincides with $\varepsilon_W^\infty(x)$ on $F_\infty(x)$ then $\varepsilon_W^\infty(x) = \varepsilon_W^\infty(y)$ and $F_\infty(y) = \{i, y_i = \varepsilon_W^\infty(x)_i\}$ (therefore $F_\infty(x) \subset F_\infty(y)$). Hence knowing the set of nodes $F_\infty(x)$ and the values of $\varepsilon_W^\infty(x)$ on that set, it is possible to reconstruct $\varepsilon_W^\infty(x)$ everywhere, for example by computing $\varepsilon_W^\infty(y)$ where $y = \varepsilon_W^\infty(x)$ on $F_\infty(x)$ and $y = 1$ everywhere else.

Particular cases

1. **G is an undirected graph with binary weights:** $w_{ij} = w_{ji} \in \{0, -\infty\}$. In this case, $\varepsilon_W^\infty(x)$ is a signal that is constant on each connected component of G, equal to the minimum of x on that connected component.

2. **G is a graph with binary weights:**$w_{ij} \in \{0, -\infty\}$. In this case, $\varepsilon_W^\infty(x)$ is a signal that is constant on each equivalence class defined by the equivalence relation $i\ j \iff w_{ij}^\infty > 0$ and $w_{ji}^\infty > 0$ (that is to say, iff there is a path from i to j and from j to i in G), and its value is equal to the minimum of x on that equivalence class. What is more, if there is a path from a node i in a class C_i to a node j in a different class C_j, then the constant value on C_i is greater than the value on C_j.

3.3.2 Openings

Granulometry $\gamma_W^{(p)} = \delta_W^p \varepsilon_W^p$ As a family of openings decreasing with p, $(\gamma_W^{(p)}), p \geq 0$ forms a granulometry: $\gamma^{(p+1)} = \delta^p \gamma \varepsilon^p \leq \delta^p \varepsilon^p = \gamma^{(p)}$ (since γ is anti-extensive). What is more, as we saw earlier, $\gamma_W^{(\infty)} = \varepsilon_W^\infty$.

Openings with changing weights Another kind of sequence of openings can be defined from a sequence $(W_n)_{n\geq 1}$ of morphological conservative weight matrices. Then starting from a signal $\mathbf{x}$ we compute a sequence of signals defined by $\mathbf{x_n} = \gamma_{W_n} \circ \gamma_{W_{n-1}} \cdots \circ \gamma_{W_1}(\mathbf{x})$.

4 Application to structure tensors

We work on the same images and use the same definitions of structure tensor and anisotropy as in Section 2.

In what folows T is a $n \times n$ image of ellipsoids (or tensors). We will index its entries by a single index. The tensor $T(i)$ is characterized by its coordinates in the image (x_i, y_i) its eigenvalues $0 \leq \lambda_2(i) \leq \lambda_1(i)$ and orhtonormal eigenvectors $e_1(i)$ and $e_2(i)$. The anisotropy at pixel i is $a_i = \frac{\lambda_1(i) - \lambda_2(i)}{\lambda_1(i) + \lambda_2(i)}$. Finally, we note θ_i the angle in $(-\frac{\pi}{2}, \frac{\pi}{2}]$ such that $e_2(i)$ is colinear to $[\cos(\theta_i), \sin(\theta_i)]^T$.

4.1 Binary matrix based on co-circularity

Here we present operators based on a binary conservative morphological weight matrix, computed as explained in Section 2.3 and 2.4. We recall the idea of this computation and provide more details.

4.1.1 Definition of W

The graph $G = (V, E)$ we consider is undericted and contains $N = n^2$ nodes. The signal x_i on node i is the anisotropy of the ellipse at pixel i. There is an edge between i and j iff the point $u_j = (x_j, y_j)$ is in a square window of fixed size $2k+1$, centered on u_i (that is, $d_{ij} \doteq ||u_i - u_j||_\infty \leq k$), and $(u_i, e_2(i))$ and $(u_j, e_2(j))$ are co-circular up to a certain angular tolerance, with the additional constraint described earlier to avoid ladder configurations - see Figure 9.

More precisely, given a point $u \in \mathbb{R}^2$ and an angle $\theta \in (-\frac{\pi}{2}, \frac{\pi}{2}]$ representing the orientation of a line passing through u, let $f_{u,\theta} : \mathbb{R}^2 \to (-\frac{\pi}{2}, \frac{\pi}{2}]$ be the function associating to each point $v \in \mathbb{R}^2$ the orientation $f_{u,\theta}(v)$ that makes (u, θ) and $(v, f_{u,\theta}(v))$ cocircular. Then we define the degree of cocircularity between nodes i and j as

$$c_{ij} = |\cos(\theta_j - f_{u_i,\theta_i}(u_j))| = |\cos(\theta_i - f_{u_j,\theta_j}(u_i))| = c_{ji}.$$

It is a number in $[0, 1]$, and the closer it is to 1, the "more cocircular" i and j are. We say that i and j are cocircular up to the angular precision $\alpha \in [0, \frac{\pi}{2}]$ if $c_{ij} \geq \cos(\alpha)$.

The additional constraint to avoid ladder configurations is also controlled by an angular parameter β. For i and j to be neighbours in G, we require that

$$\max(b_{ij}, b_{ji}) \geq \cos(\beta),$$

with the following definition of b_{ij}

$$b_{ij} \doteq \left|\frac{\overrightarrow{u_i u_j}}{||\overrightarrow{u_i u_j}||} \cdot e_1(j)\right|.$$

As shown in Figure 9, this restricts the space of possible neighbours to a kind of double cone. We will therefore refer to this constraint as the "conic constraint".

Finally, the adjacency matrix W is defined by $w_{ij} = 0$ if the two constraints are fullfilled or if $i = j$, and $w_{ij} = -\infty$ otherwise. Noting $\tilde{b}_{ij} = \mathbb{1}_{[\cos(\beta),1]}(\max(b_{ij}, b_{ji}))$, $\tilde{c}_{ij} \doteq \mathbb{1}_{[\cos(\alpha),1]}(c_{ij})$ and $\tilde{d}_{ij} = \mathbb{1}_{[0,2k+1]}(d_{ij})$, we can also write for $i \neq j$

$$w_{ij} = \log(\tilde{b}_{ij} \cdot \tilde{c}_{ij} \cdot \tilde{d}_{ij}).$$

Hence, here W depends on the variables $(x_i, y_i, \theta_i)_{1 \leq i \leq N}$, but not on $\lambda_1(i)$ and $\lambda_2(i)$.

4.1.2 Granulometry $\gamma_W^{(p)}$

Figure 11 shows the result of openings $\gamma_W^{(p)}$ (as defined in Section 3.3.2) on an anisotropy image. The bright parts (high anisotropy) vanish first in the background, that is to say outside the vessels, but even the vessels eventually disappear. This is due to the fact that the graph G is connected (it has only one connected component). This kind of results motivates the search for an operator that would converge towards an anisotropy image where the brightness is preserved in the vessels but not in the background.

4.2 Non binary matrix including anisotropy information

The original motivation for including anisotropy in the definition of W was to apply a new opening on a tensor field resulting from a previous opening.

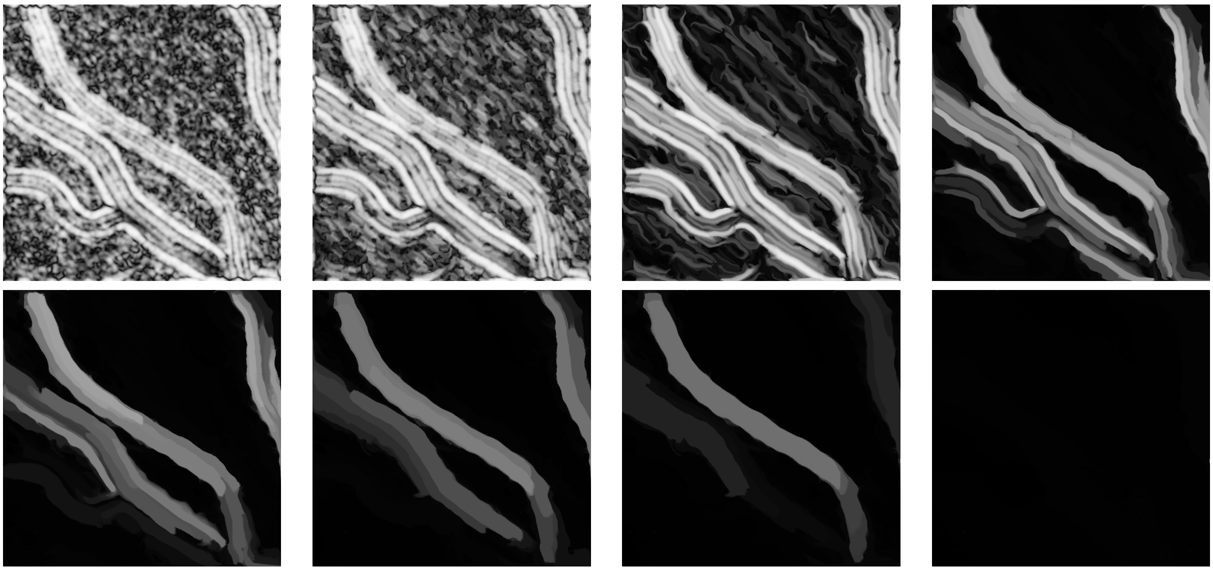

Figure 11: Example of openings $\gamma_W^{(p)}$ on an anisotropy image, in the case of a binary and symmetric matrix W, computed as explained in Section 4.1.1. From left to right, top to bottom: $p = 0$ (original anisotropy image), $p = 1, 5, 15, 20, 30, 40, 60$. The parameters used here are $k = 7$ (spatial window), $\alpha = \frac{\pi}{20}$ (cocircularity precision) and $\beta = \frac{\pi}{6}$ (conic constraint).

4.2.1 Definition of W

We use the same notations as in Section 4.1.1. In addition, a_i and a_j denote the anisotropy at pixels (or nodes) i and j. Then as before we set $w_{ii} = 0$, and for $i \neq j$

$$\begin{cases} \tilde{w}_{ij} & = & \tilde{d}_{ij} \cdot \tilde{b}_{ij} \cdot \max\left(\sqrt{c_{ij} \cdot \min(a_i, a_j)}, 1 - a_i\right)^{1/4} \\ w_{ij} & = & \log(\tilde{w}_{ij}). \end{cases}$$

Not only W is now non-binary ($a_i, a_j, c_{ij} \in [0,1]$), but it is also asymmetric. Indeed, the idea is that a node with low anisotropy value should have a strong effect on its spatial neighbourhood during the erosion (that is the meaning of $\max(., 1 - a_i)$); and a node which had originally a large anisotropy and is cocircular with other bright nodes, should recover a large value during dilation if it has been darkened during erosion (that is the meaning of $\max(\sqrt{C_{ij} \cdot \min(a_i, a_j)}, .)$). The power $1/4$ was set empirically to see significant effects of erosion and dilation.

Here W depends on the whole information containes in T: it depends on the variables $(x_i, y_i, \theta_i)_{1 \leq i \leq N}$ and also on $\lambda_1(i)$ and $\lambda_2(i)$ through the anisotropy a_i. We note g the function that associates W to these variables, that is: $W = g(u, \theta, a)$ where $u = (x_i, y_i)_{1 \leq i \leq N}$, $\theta = (\theta_i)_{1 \leq i \leq N}$ and $a = (a_i)_{1 \leq i \leq N}$.

4.2.2 Granulometry $\gamma_W^{(p)}$

See Figure 12.

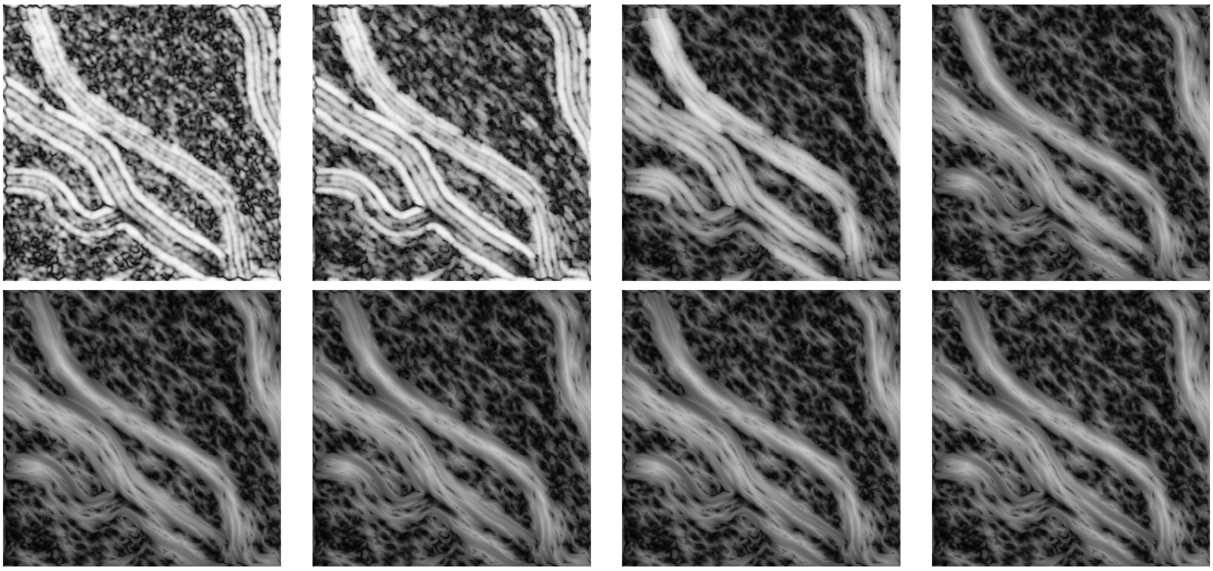

Figure 12: Example of openings $\gamma_W^{(p)}$ on an anisotropy image, in the case of a non-binary and non symmetric matrix W, computed as explained in Section 4.2. From left to right, top to bottom: $p = 0$ (original anisotropy image), $p = 1, 5, 15, 20, 25, 30, 37$. The value $p = 37$ is the p_{max} for W. The parameters used here are $k = 7$ (spatial window), $\alpha = \frac{\pi}{20}$ (cocircularity precision) and $\beta = \frac{\pi}{6}$ (conic constraint).

4.2.3 Openings with changing weights

Starting from $T = (u, \theta, a, \lambda_1 + \lambda_2)$ we define a sequence by $a_0 = a$, $W_0 = g(u, \theta, a_0)$, and then

$$\begin{cases} a_{n+1} &= \gamma_{W_n}^{(p)}(a_n), \\ W_{n+1} &= g(u, \theta, a_{n+1}). \end{cases}$$

An example of results is shown on Figure 13.

References

[1] Tsuyoshi Ando. *Problem of Infimum in the Positive Cone*, pages 1–12. Springer Netherlands, Dordrecht, 1999.

[2] Bernhard Burgeth, Andres Bruhn, Nils Papenberg, Martin Welk, and Joachim Weickert. Mathematical morphology for matrix fields induced by the Loewner ordering in higher dimensions. *Signal Processing*, 87(2):277 – 290, 2007. Tensor Signal Processing.

[3] Alejandro F Frangi, Wiro J Niessen, Koen L Vincken, and Max A Viergever. Multiscale vessel enhancement filtering. In *International Conference on Medical Image Computing and Computer-Assisted Intervention*, pages 130–137. Springer, 1998.

[4] Richard V. Kadison. Order properties of bounded self-adjoint operators. *Proceedings of the American Mathematical Society*, 2(3):505–510, 1951.

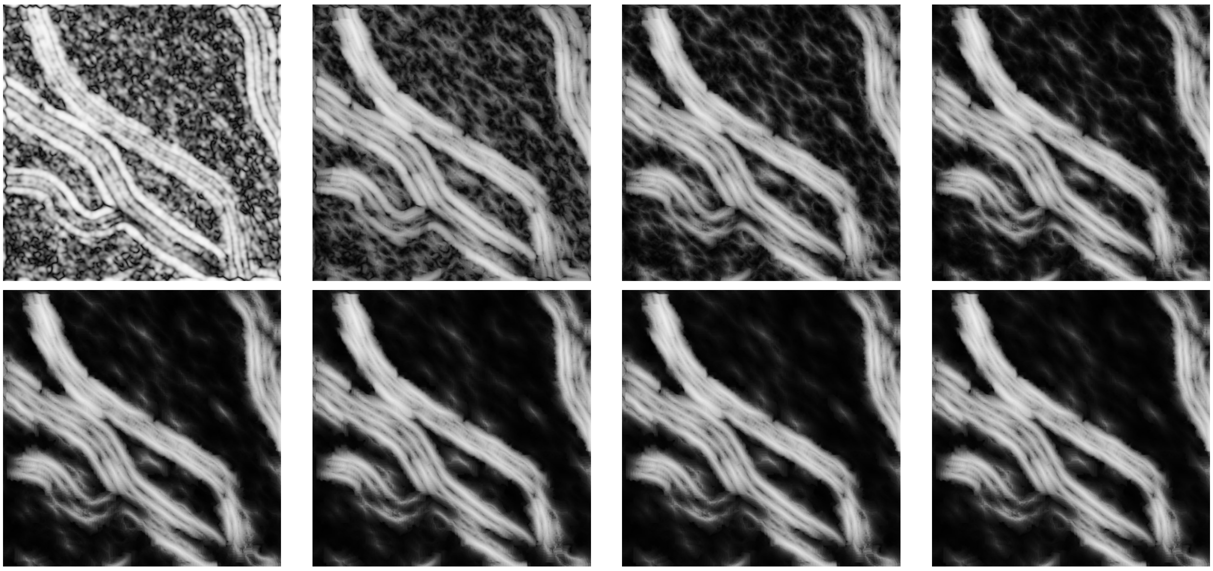

Figure 13: Sequence of anisotropy images defined as in Section 4.2.3. In this example $p = 4$, and from left to right, top to bottom: $n = 0$ (original anisotropy image), $n = 1, 2, 3, 5, 7, 10, 13$. After $n = 13$, no significant change occurs.

[5] T. Moreland and S. Gudder. Infima of hilbert space effects. *Linear Algebra and its Applications*, 286(1):1 – 17, 1999.

[6] Jasper Joris van de Gronde. *Beyond Scalar Morphology: A Theoretical Framework for Mathematical Morphology on Colour and Tensor-valued Images*. University of Groningen, 2015.

[7] Santiago Velasco-Forero and Jesús Angulo. *Nonlinear Operators on Graphs via Stacks*, pages 654–663. Springer International Publishing, Cham, 2015.